Iran. J. Radiat. Res., 2011; 9(1): 29-36

Evaluation of the electron energy fluence and angular distributions from a clinical accelerator. A BEAMnrc Monte Carlo study

N. Jabbari[1*], H. Nedaie[2], A. Zeinali[1]

[1]Department of Medical Physics and Imaging, Urmia University of Medical sciences, Urmia, Iran
[2]Department of Radiotherapy, Cancer Institute, Tehran university of Medical Science, Tehran, Iran

Background: Understanding of the incident electron energy and angular distributions from clinical electron accelerators (linacs) is important for dosimetry and treatment planning. The most important goals of this study were to evaluate the energy fluence and angular distributions of electron beams from a Neptun 10PC linac using the Monte Carlo (MC) code. ***Materials and Methods:*** The linac electron beams (6, 8, and 10 MeV) were modeled, using the BEAMnrc MC system based on the Electron-Gamma-Shower (EGSnrc) code. Central axis depth-dose curves and dose profiles of the electron beams were measured experimentally, and calculated with the MC for three field sizes. In order to benchmarking the simulated models, the calculated and measured dose distributions were compared with Kolmogorov–Smirnov (KS) statistical test. ***Results:*** The KS test indicated that the calculated percent depth dose (PDD) and dose profile values for the three electron beam energies well agree with measured data (within 2% everywhere). The results also showed good agreement (discrepancies smaller than 1%) between the simulated electron energy parameters and those calculated from energy-range relationships using equations for the reference field size. ***Conclusion:*** The results showed that there was no significant difference between energy fluence curves of each electron beam energy at different field sizes. In addition, the results of the calculated angular distributions showed that the direction of the electron emerged from the treatment head and trimmer applicators were in forward direction. **Iran. J. Radiat. Res., 2011; 9(1): 29-36**

Keywords: *Linac, electron beam, energy fluence, angular distribution, Monte Carlo.*

INTRODUCTION

Nowadays, electron therapy plays an important role in radiation therapy. The most clinically useful energy range for electrons is 6 to 20 MeV. Electron beams are commonly used in the treatment of skin, lip cancer, chest-wall, neck cancers, upper respiratory and digestive-tract lesions from 1 to 5 cm in depth, boost treatment to lymph nodes, operative scars and residual tumor. Clinically, the most important quantity to calculate in radiotherapy is the dose distribution per monitor unit in patients undergoing cancer treatment by ionizing radiation. Optimizations of the therapeutic gain of radiation, i.e. maximizing the dose to tumors, while minimizing the dose to healthy tissues, critically depend on the accuracy of the dose calculation [1, 2].

The dosimetric properties of electron beams produced by modern radiotherapy treatment machines vary among the manufacturers, mostly due to differences in the treatment-head design. Even linacs produced by the same manufacturer can have different beam characteristics (energy spectrum and angular distribution) [3].

Understanding of the incident electron energy and angular distributions from clinical electron accelerators (linacs) is important for dosimetry and treatment planning [4, 5]. The electron energy spectrum has a dominant effect on the central axis depth dose curves [6].

Many researches have documented the effects of treatment machine beam collimation systems on the output factors and the electron beam characteristics on the dose distributions [7-10]. Some investigations have been carried out for various electron beam energies and applicator sizes to study

Corresponding author:
Dr. Nasrollah Jabbari,
Department of Medical Physics and Imaging, Faculty of Para medicine, Urmia University of Medical Sciences, Urmia, Iran
Fax: *+98 441 2770047*
E-mail: *njabbarimp@gmail.com*

the contribution of the photon dose to the final central axis depth doses [11, 12].

In an attempt to calculate dose to the patient more accurately, 3D planning algorithms were developed which required the initial phase-space (IPS), as input file just below the electron applicator [13, 14]. The IPS is a distribution in position, energy and direction of electrons and photons in a plane in front of the patient [15]. One approach to determine the electron beam character is to simulate the transport of particles through the treatment head, using the MC technique [16]. The MC is, potentially, the most accurate method for the calculation of radiation dose if the radiation source and machine geometry model accurately and also sufficiently large number of particle histories be run [17, 18]. The Monte Carlo method also has shown considerable accuracy in dose calculations for small field sizes [19].

The application of the Monte Carlo method to the simulation of electron beams has a long history. Udale-Smith used MC calculations to show how the quantitative details of the energy and angular distributions incident on the patient plane, especially including electrons having undergone large-angle scattering or highly inelastic collision, affect the shape of electron depth dose curves [20].

Any planning system requires the ability to perform accurate dose calculations. Since electron transport and scatter in matter is strongly influenced by density and material composition, dose calculation in heterogeneous media is extremely challenging [21]. Nonetheless, the MC simulations are better suited to include the effects of low energy electrons scattered through large angles from the central axis. There are different MC codes for simulation of photons, electrons and the coupled transport of electrons and photons but they use different physical theories [22].

The current study is based on computer simulations of the Neptun 10PC linac treatment head and a water phantom, drawing on detailed analysis of the phase-space of simulated beams. So, the main objectives of this work were: a) to determine the electron energy fluence distributions, b) to determine the electron angular distribution forms c) to determine the mean and most probable energies for the electron beams of this linac.

MATERIALS AND METHODS

Medical linear accelerator

The modeled linac was NEPTUN 10PC medical linear accelerator which is made in Poland. The accelerator was a stationary wave type equipped with an achromatic bending magnet system. The linac provided photon and electron beams irradiation. In this investigation, the configurations of 6, 8 and 10MeV electron beams were studied. The electron applicators of this linac were variable trimmers consisting of five scrappers. Every scrapper was constructed from 3 layers with different thickness and materials. The distances between all the scrapers were the same, except for the last one. In order to achieve a flat dose profile and patient comfort, all experimental measurements, as well as simulated calculations were carried out at a source to surface distance (SSD) of 105 cm. Detailed information of the geometry and materials of the applicators was provided by the vendor.

Experimental measurements

The central axis depth dose curves were measured at SSD = 105 cm using a computerized water phantom radiation field analyzer (Scanditronix RFA-300 – IBA Scanditronix Medical AB, Uppsala, Sweden). A waterproof high doped p-type silicon diode (EFD-3G, made by the same manufacturer) was used to measure the percentage of depth doses at the central axis. The thickness of the silicon chip was 0.5 mm and its' active area diameter is 2 mm. Another diode was placed in the corner of the radiation field during the experimental measure-

ments as the reference detector. The PDD curves for 6, 8 and 10 MeV electron beams were measured with trimmers in the place for three field sizes (3 × 3, 10 × 10, 25 × 25 cm^2). In addition, the dose profiles were measured for the reference field size (10 × 10 cm^2) at the d_{max} for each electron beam.

Monte Carlo calculations

The electron beams were modeled using the BEAMnrc codes. Detailed geometry and materials of various components of the linac was provided by the vendor [23]. Three field sizes (3 × 3, 10 × 10 and 25 ×25 cm^2) and three nominal electron beam energies (6, 8 and 10 MeV) at SSD = 105 cm were modeled. The electron nominal energies were considered as monoenergetic parallel circular beam sources with a 2 mm diameter incident size.

The electron beam energies were adapted to give depth dose curves having the same depth at 50% dose level. For all simulations, the energy cut-offs for the electron transport were set to ECUT (electron cut-off energy) = 0.7 MeV (kinetic energy plus rest mass) and PCUT (photon cutoff energy) = 0.01 MeV. Enough number of electrons histories (10^8) were ran to achieve 1% relative standard error of the mean of the calculated dose. The particles, after being transported, were scored at a scoring plane placed at the bottom of the last scraper.

The information of the scoring plane, which has conventionally been named the phase space file by the code, was used as the source input for the simulations of the dose distributions in the water phantoms of a rectilinear voxel geometry configuration using the DOSXYZnrc system being based on the EGSnrc Monte Carlo code [24]. Statistical uncertainties of a Monte Carlo simulation could simply be reduced by running more particle histories, so that its effect became insignificant for a particular application [25]. Therefore, by using 10^8 histories the statistical uncertainties, obtained by the EGSnrc Monte Carlo simulation code in this study, was estimated to be about 0.5% and 1% for the phase-space parameters and the absorbed dose calculation, respectively.

In order to benchmark the simulated models, the PDD curves and dose profiles at dmax were also measured experimentally for all the energy settings at the reference field size with the diode detectors in the RFA 300 water phantom, as mentioned above. The calculated values obtained by MC were compared and tested against the measured values using the Kolmogorov–Smirnov statistical test. After the bench-marking, the central axis depth-dose curves of the electron beams for the smallest and largest field sizes (3×3 cm^2 and 25×25 cm^2) were measured and calculated.

The BEAMDP (BEAM Data Processor) system was used to analyze the phase-space files and determine the electron energy fluence and electron angular distributions. The interval energy bins was set to 0.05 MeV and the number of angular bins was set at 180, and the minimum and maximum angles were also set to 0 and 90, degrees respectively. Furthermore, the most probable energy Ep_o and mean energy E_0 was determined by the Monte Carlo simulated phase-spaces.

The established empirical relation between the beam characteristics at the phantom surface, and the depth–dose distribution for electron beams were also investigated. The most probable energy at the phantom surface Ep_o could be determined by the depth of the practical range Rp in water using the equation 1 [26]:

$$Ep_o = 0.22 + 1.98Rp + 0.0025Rp^2 \qquad (1)$$

Another energy of interest for dosimetry purpose was the mean energy on the phantom surface E_0, which was determined by the R_{50}, the depth at which the dose fell to 50% of the maximum dose, using the equation 2 [24]:

$$E_0 = 2.33R_{50} \qquad (2)$$

In this study the Monte Carlo simulated

depth–dose ranges R_{50} and Rp were applied to equations 1 and 2 for calculations of Ep_0 and E_0 respectively. The values of the Ep_0 and E_0, were also extracted from the Monte Carlo simulations.

RESULTS

The main function of the BEAMnrc calculations was to generate a variety of phase-space data files that were used as input source files for the DOSXYZnrc program to calculate dose distributions in a water phantom, and to create a basis on which the multiple-source models can be built. The phase-space data files derived from the MC simulation of the linac were used for the calculated values. The statistical uncertainty of the results presented was ±1% for depth-dose values, and less than ±2% for the profile data calculated in the homogeneous water phantom. The central axis depth-dose and dose profile values calculated from the BEAMnrc phase-space data files were compared with those measured experimentally. Figure 1 shows the measured and calculated depth dose curves for the linac electron beams (6, 8, and 10 MeV) in the reference field (10×10 cm²). Figure 2 shows the measured and calculated dose profiles at the d_{max} for the three electron beam energies at the reference field size. The measured and calculated PDD and dose profile curves were in agreement within 1 and 2 mm respectively. The Kolmogorov-Smirnov test indicated that the calculated PDD and dose profile values for the three electron beam energies were in good agreement with measured data (within 2% everywhere).

Figures 3 and 4 show the measured and calculated depth-dose curves obtained for the 6, 8, and 10 MeV electron beams in the smallest (3 × 3 cm²) and largest (25 × 25 cm²) field sizes.

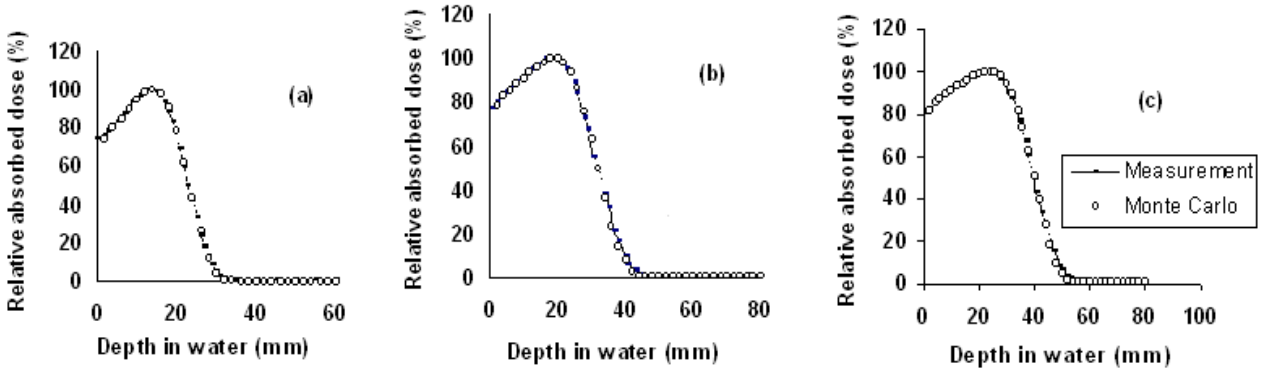

Figure 1. Central axis PDD curves of the experimental measurements and MC calculations for different electron beam energies of the linac: 6MeV (a), 8MeV (b) and 10MeV (c), at the reference field size (10×10 cm²).

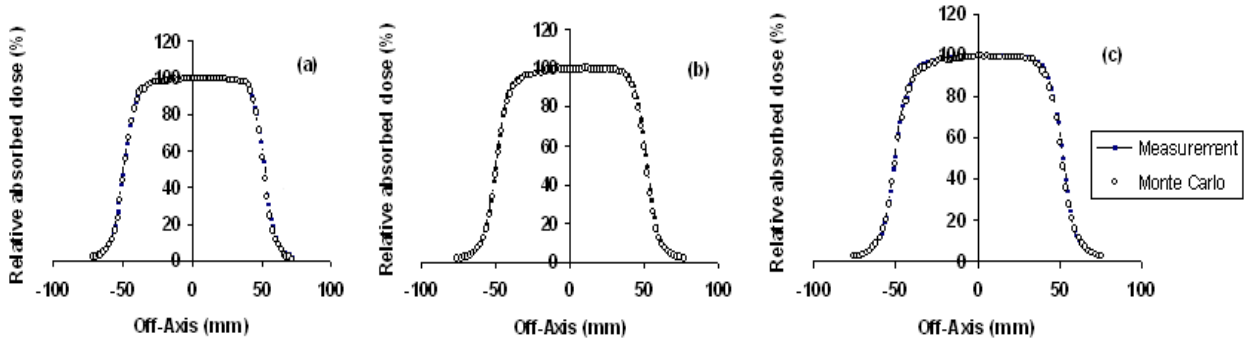

Figure 2. Dose profiles of the experimental measurements and MC calculations for different electron beam energies of the linac: 6MeV (a), 8MeV (b) and 10MeV (c), at the reference field size (10×10 cm²).

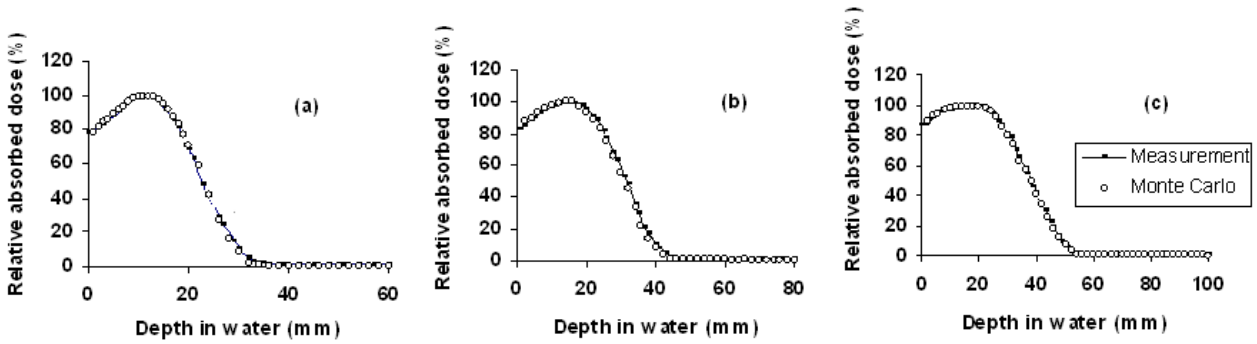

Figure 3. Central axis PDD curves of the experimental measurements and MC calculations for different electron beam energies of the linac: 6 MeV (a), 8 MeV (b) and 10 MeV (c), at the smallest field size (3 × 3 cm²).

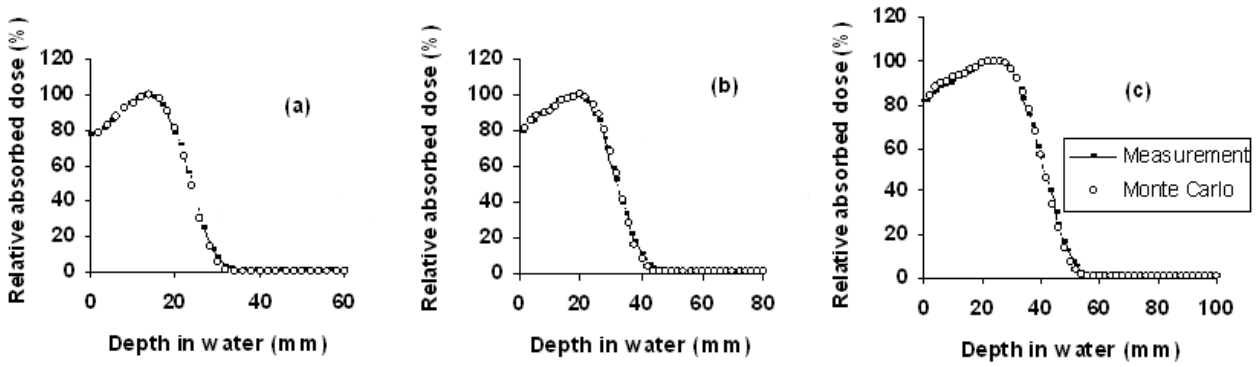

Figure 4. Central axis PDD curves of the experimental measurements and MC calculations for different electron beam energies of the linac: 6 MeV (a), 8 MeV (b) and 10 MeV (c), at the largest field size (25 × 25 cm²).

Energy fluence distributions and parameters

Figure 5 shows the calculated of the energy fluence for the monoenergetic initial beams of the NEPTUN linac at the scoring plane. All the electron energy fluence curves were normalized to their most probable energy. In figure 5(a) it can be seen that the peak values of the curves indicate that the highest electron energy fluence distribution for the 6 MeV electrons beam at three field sizes had been located at the 5.8 to 5.95 MeV ranges. Figures 5(b) and 5(c) also show that the peak values for 8 and 10 MeV electron beams at three field sizes were located at 7.75 to 7.95 MeV and 9.8 to 9.95 MeV, respectively. It can be seen that there has not been any significant difference between the curves of electron beam energy at different field sizes.

The Monte Carlo simulated depth–dose ranges R_{50} and R_p were applied to equations 1 and 2 for calculations of E_{p0} and E_0 respectively for the reference field size at the phantom surface (SSD=105cm). In table 1, the result is compared with the corresponding energy parameters extracted from the Monte Carlo simulated phase-spaces. A comparison of the extracted values and those calculated according to equations showed that the best agreements had been achieved.

Table 1. A comparison of simulated electron energy parameters and those calculated from energy-range relationships using equations 1 and 2 for the reference field size.

	Most probable energy (MeV)		Mean energy (MeV)	
Electron beam energy (MeV)	Simulated	Equation (1)	Simulated	Equation (2)
6	6.20	6.16	5.67	5.70
8	8.25	8.22	7.45	7.49
10	9.93	9.90	9.30	9.35

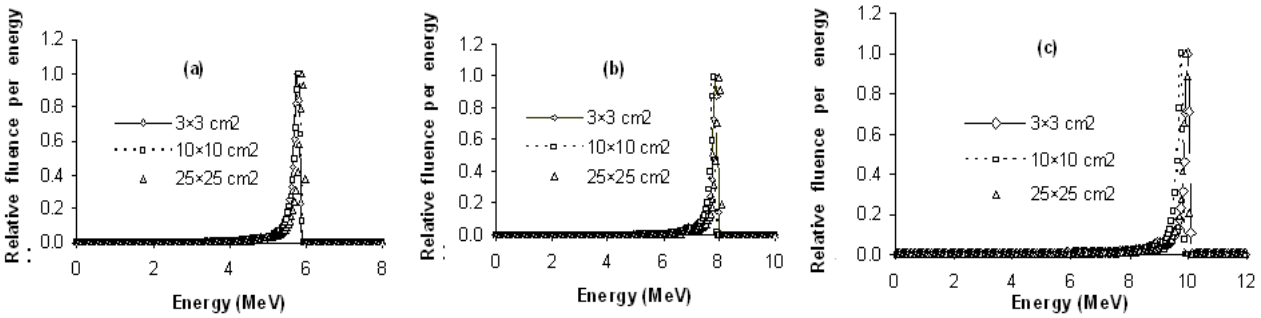

Figure 5. The electron energy fluence for different electron beam energies of the linac: 6 MeV (a), 8 MeV (b) and 10 MeV (c), at the scoring plane for three field sizes.

Angular distributions

The angular distributions of the electron beams at a scoring plane after the last scraper (SSD=100cm) for three field sizes are shown in figure 6. The curves were normalized to the most probable scattering angles. As it could be noted from the figure, the peak values of the curves indicated that the highest electron angular distribution for the 6, 8, and 10 MeV at three field sizes were located in the angular range of 0.5 to 3.5 degrees. This proved that the direction of the electron emerged from the treatment head and trimmer applicators were in forward direction. It also indicated that the electrons are transported in a rather smaller angle with increasing the electron energy.

DISCUSSION

The results of this study showed that the MC calculated PDD, and does profile curves matched well with the experimentally measured ones (within 2%). Our findings also indicated that the agreement between the values of the most probable electron energy at the phantom surface (Ep_0), and the mean energy on the phantom surface (E_0) was extracted by the Monte Carlo data and calculated from the equations of 1 and 2 (within 1%) in all cases . Ding *et al.* [27] have used Monte Carlo simulations to study the relation between E_0 and R_{50} for a variety of beams from different medical accelerators with an energy range of 5–50 MeV. They found that equation (2) slightly overestimated the mean energy of electron beams from accelerators with scattering foil. These proved the validity of the MC simulation method used in this study for the determination of the electron beam characteristics (energy fluence and angular distribution).

The beam characteristics are usually different due to the variation in accelerator designs and on-site beam tuning. The results showed that there was no significant difference between energy fluence curves of the each electron beam energy at different

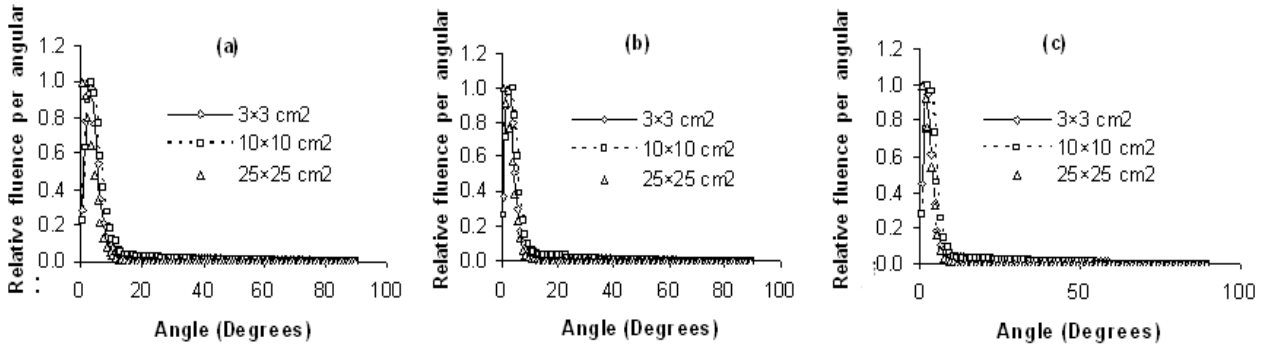

Figure 6. The angular distributions for different electron beam energies of the linac: 6 MeV (a), 8 MeV (b) and 10 MeV (c), at the scoring plane for three field sizes.

field sizes. It was also noted that the energy fluence at the scoring plane had fewer low-energy electrons. This can be explained by the fact that the energy spectra at the scoring plane were strongly dependent on the details of the accelerator tube tuning characteristic being already pointed out by Jabbari *et al.* [28]. Furthermore, Deasy *et al.* [29] and Kok and Welleweerd [30] have also found that the energy fluence were only affected moderately by the scattering foil design, as the scattering foil thickness could not account for the width or the shapes for the different energies.

The results of calculated angular distributions showed that the direction of the electron emerged from the treatment head and trimmer applicators were in forward direction. It also indicated that the electrons are transported in a rather smaller angle with increasing the energy of the electron beams. Deasy *et al.* [26] and Bjork *et al.* [9] showed that the angular distribution was mainly affected by the passage of the electrons through the scattering foil system. This indicates that the angular distribution should be fairly independent of energy spectral variations within reasonable limits. Since all beams were transported through the same accelerator geometry, there should not be any significant differences between the various electron beams.

It is again emphasized that the energy fluence presented in this study were for the forward-going electrons only; therefore it widely neglected the scattered components. Further, the quantitative progress at this point was required, so that, the energy distribution to be a crucial parameter in Monte Carlo treatment planning with linear accelerators having a considerable energy spread.

REFERENCES

1. Hogstrom KR and Almond PR (2006) Review of electron beam therapy physics. *Phys Med Biol, **51**: R455-R489.*
2. Khan FM (2003) The physics of radiation therapy, 3rd ed. Lippincott Williams and Wilkins, Philadelphia
3. Antolak JA, Bieda MR, Hogstrom KR (2002) Using Monte Carlo methods to commission electron beams: A feasibility study. *Med Phys, **29**: 771-786.*
4. Ding GX, Rogers DWO, Makie TR (1995) Calculation of stopping-power ratios using realistic clinical electron beams. *Med Phys, **22**: 489-501.*
5. Rogers DWO, Faddegon BA, Ding GX, Ma CM Wei J, Makie TR (1995) BEAM: A Monte Carlo code to simulate radiotherapy treatment units. *Med Phys, **22**: 503-524.*
6. Deng J, Jiang SB, Pawlicki T, Li J, Ma CM (2001) Derivation of electron and photon energy spectra from electron beam central axis depth dose curves. *Phys Med Biol, **46**: 1429-1449.*
7. Kapur A, Ma CM, Mok EC, Findley DO and Boyer AL (1998) Monte Carlo calculations of electron beam output factors for a medical linear accelerator. *Phys Med Biol, **43**: 3479 – 3494.*
8. Choi MC, Purdy JA, Gerbi B, Abrath FG, Glasgow GP (1979) Variation in output factor caused by secondary blocking for 7-16 MeV electron beams. *Med Phys, **6**: 137-139.*
9. Bjork P, Knoos T, Nilsson P (2004) Measurments of output factors with different detector types and Monte Carlo calculations of stopping – power ratios for degraded electron beams. *Phys Med Biol, **49**: 4493 – 4506.*
10. Keall PJ and Hoban PW (1994) The angular and energy distribution of the primary electron beam. *Australas Phys Eng Sci Med, **17**: 116–23.*
11. Klevenhagen SC (1994) An algorithm to include the bremsstrahlung contamination in the determination of the absorbed dose in electron beams. *Phys Med Biol, **39**: 1103 – 1112.*
12. Sorcini BB, Hyodynmaa S, Brahme A (1996) The role of phantom and treatment head generated bremsstrahlung in high – energy electron beam dosimetry. *Phys Med Biol. **41**: 2657 – 2677.*
13. Janssen JJ, Korevaar EW, Storchi PRM, Huizenga H (1997) Numerical calculation of energy deposition by high-energy electron beams: III-B. Improvements to the 6D phase space evolution model. *Phys Med Bio, **42**: 1441–9.*
14. Kawrakow I, Fippel M, Friedrich K, (1996) 3D electron dose calculation using a voxel based Monte Carlo algorithm (VMC). *Med Phys, **23**: 445–57.*
15. Janssen JJ, Korevaar EW, Storchi PRM, Huizenga H (2001) A model to determine the initial phase space of a clinical electron beam from measured beam data. *Phys Med Biol, **46**: 269–286.*
16. Ma CM. Faddegon BA, Rogers DWO, Mackie TR (1997) Accurate characterization of Monte Carlo calculated electron beams for radiotherapy. *Med Phys, **24**: 401-416.*
17. Ma CM and Jiang SB (1999) Monte Carlo modeling of electron beams from medical accelerators. *Phys Med Biol, **44**: R157–R189.*
18. Mesbahi A (2006) Development a simple point source model for Elekta SL-25 linear accelerator using MCNP4C Monte Carlo code. *Iran J Radiat Res, **4**: 7-14.*
19. Mesbahi A (2008) The effect of electronic disequilibrium on the received dose by lung in small fields with photon beams: Measurements and Monte Carlo study. *Iran J Radiat Res, **6**: 70-76.*

20. Udale-Smith M (1992) Monte Carlo calculations of electron beam parameters for three Philips linear accelerators. *Phys Med Biol,* **37**: 85-105.
21. Lee MC, Deng J, Li J, Jiang SB, Ma CM (2001) Monte Carlo based treatment planning for modulated electron beam radiation therapy. *Phys Med Biol,* **46**: 2177–2199.
22. Nedaie H, Shariary M, Gharaati H, Allahverdi M, Mosleh-Shirazi MA (2005) Comparison of MCNP4C, 4B and 4A Monte Carlo codes when calculating electron therapy depth doses. *Iran J Radiat Res, **2**: 191-195.*
23. Andrzej Sołtan Institute for Nuclear Studies, 05-400 Swierk/Otwock, Poland. www.hitecpoland.eu
24. Walters B, Kawrakow I, Rogers DWO (2006) DOSXYZnrc users manual. NRCC Report PIRS-794 (rev. B). NRCC, Ottawa.
25. Ma CM, Li JS, Jiang SB et al. (2005) Effect of statistical uncertainties on Monte Carlo treatment planning. *Phys Med Biol*, ***50**: 891–907.*
26. American Association of Physicists in Medicine (AAPM) Task Group 25 (1991) Clinical electron-beam dosimetry. *Med Phys*, ***18**: 73–109.*
27. Ding GX, Rogers DWO, Mackie TR (1996) Mean energy, energy–range relationships and depth-scaling factors for clinical electron beams. *Med Phys*, ***23**: 361–76.*
28. Jabbari N, Hashemi-Malayeri B, Farajollahi A, Kazemnejad A, Shafaie A, Jabbari S (2007) Comparison of MCNP4C and EGSnrc Monte Carlo codes in depth-dose calculation of low energy clinical electron beams. *J Phys D: Appl Phys, **40**: 4519–4524.*
29. Deasy JO, Almond PR, McEllistrem MT (1996) Measured electron energy and angular distributions from clinical accelerators. *Med Phys*, ***23**: 675–684.*
30. Kok JG and Welleweerd J (1999) Finding mechanisms responsible for the spectral distribution of electron beams produced by a linear accelerator. *Med Phys*, ***26**: 2589–2596.*